Perpendicular anisotropy detected by transversely biased initial susceptibility via the magneto-optic Kerr effect in Fe_xSi_{1-x} thin films and Fe_xSi_{1-x}/Si multilayers: Theory and experiment

L. M. Alvarez-Prado, G. T. Pérez, R. Morales, F. H. Salas,* and J. M. Alameda
Laboratorio de Magnetoóptica y Láminas Delgadas, Departamento de Física, Universidad de Oviedo, c/ Calvo Sotelo, s/n, E-33007 Oviedo, Spain
(Received 20 September 1996; revised manuscript received 13 February 1997)

We studied experimentally and theoretically the perpendicular anisotropy and the stripe-domain structure in both Fe_xSi_{1-x} thin films and Fe_xSi_{1-x}/Si multilayers, the latter being in the low-modulation-length regime ($0.4\ \text{nm}<\lambda<7\ \text{nm}$). The experimental study was made by means of the transversely biased initial susceptibility $\chi_{t\beta}$ via the magneto-optic Kerr effect. The samples under study were prepared by dc triode sputtering at $T_S=300$ K. It is found that the appearance of stripe domains is more pronounced for decreasing λ as x remains constant and may be caused by both the increase in effective magnetic thickness and the reduction in effective magnetization as λ decreases. For multilayers with $\lambda=0.4$ nm, the observed field dependence of $\chi_{t\beta}^{-1}$ is similar to that found in *homogeneous* thin films when weak stripe-domain structures arise as a consequence of the existence of perpendicular anisotropy K_N. We propose a quasistatic one-dimensional model to explain the behavior of $\chi_{t\beta}^{-1}$ when stripe domains are present, and we analyze the critical occurrence of stripe domains. We calculated the so-called *pseudo-uniaxial anisotropy field* H_{Ks}, associated with the stripes, in two extreme cases: exchange-driven susceptibility or magnetic free poles (nonzero divergence in the bulk). The latter case agrees better with experiment. We found that perpendicular anisotropy is *not* exclusive of a well-defined multilayer structure; i.e., K_N arises even when there are no interfaces in the volume. By setting the experimental saturation field H_s (obtained by hysteresis loops) into our model, we obtain both the perpendicular anisotropy constant $K_N=10^4-10^5$ J/m^3 and the critical thickness t_c for the occurrence of a stripe-domain structure. Some possible sources of perpendicular anisotropy are discussed, for example, the associated isotropic compressive stress σ, whose contribution is found to be $|K_N|_{\text{magnetoel}}\approx 1.5-4.5\times 10^4$ J/m^3. [S0163-1829(97)07730-8]

I. INTRODUCTION

The correct concept of *magnetic-domain structures* was discussed by Landau and Lifshitz,[1] who calculated the size of magnetic domains by considering the magnetostatic energy. Other important contributions were made by Kennard,[2] Néel,[3] and Kittel.[4] Later, some of these calculations were confirmed experimentally by Williams, Bozorth, and Shockley[5] on single crystals of silicon iron.

It is well known that magnetic thin films having perpendicular anisotropy K_N can show a peculiar domains structure known as *stripe-domain*[6,7] structure. Such films are characterized by having the normal component of the magnetization vector pointing up and down alternately with its tangential part in a direction parallel to the resultant magnetization.[6] The stripe-domain Bitter pattern was observed by Spain[8] and Saito, Fujiwara, and Sugita.[9] Likewise, the inner variation of the magnetization was verified by electron microscopy by Koikeda, Susuki, and Chikazumi.[10] Stripe-domain films can arise, even when $K_N<2\pi M_s^2$, for a film thickness larger than a critical value[6,9,11] $t_c(K_N, M_s)$, while, below this value of film thickness, M will lie in the film plane. Because of the tilted M, the hysteresis loops of this kind of film have a peculiar shape, called *transcritical*,[12–15] showing low remanence in zero applied field. Both the transcritical hysteresis loop and the width of the stripes depend on the film thickness, so that below t_c the stripe-domain structure and the transcritical loop disappear and the magnetization lies (because of the dominant shape anisotropy) in the film plane. In the presence of stripe domains, the behavior of the average in-plane magnetization has been explained assuming a pseudo-uniaxial anisotropy (*rotatable anisotropy*[11,16]) in the film plane whose easy axes were along the stripe domains.

From the experimental point of view, the technique of transversely-biased initial susceptibility[17] (TBIS) $\chi_{t\beta}$ [measured via the magneto-optic Kerr effect[18] (MOKE)] is a very sensitive and powerful method for determining and relating to each other both macroscopic and local anisotropy fields in amorphous and crystalline films and alloys.[18–20]

In fact (as explained below), the inverse TBIS ($\chi_{t\beta}^{-1}$) is proportional to the effective field acting on the average in-plane magnetization. Thus TBIS is a suitable method for the study of the stripe-domain contribution to the effective field; this contribution is given through the above-mentioned field H_{Ks}.

In the past few years, the system made of FeSi/Si in its multiple forms, e.g., amorphous, polycrystalline, and epitaxial thin films, iron disilicides, multilayers, superlattices, etc., has drawn immense attention in the magnetism community,[15,19,21–33] leading to a better understanding of interesting phenomena, as for example, the possibility of having antiferromagnetic interlayer coupling in FeSi/Si. Likewise, TBIS measurements also have evidenced the existence of different magnetic phases[21] in Fe_xSi_{1-x}/Si multilayers for

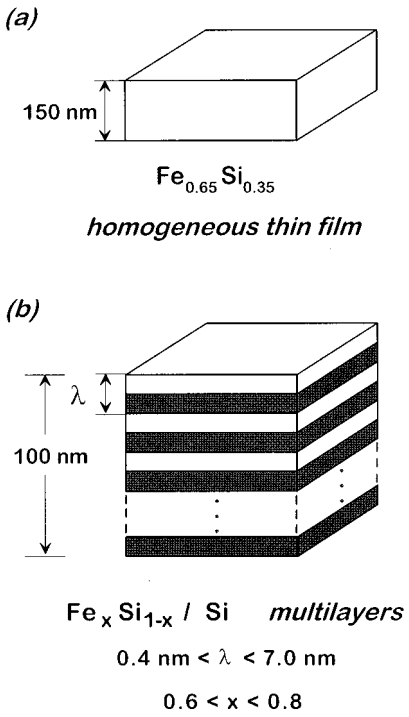

FIG. 1. Magnetic systems studied. λ refers to the modulation length.

1.2 nm$<\lambda<$3.5 nm with $0.60<x<0.80$.

In this article we study both experimentally and theoretically the field dependence of $\chi_{t\beta}^{-1}$ in both Fe_xSi_{1-x} thin films and Fe_xSi_{1-x}/Si multilayers, the latter with very low values of *nominal* modulation length ($0.4<\lambda<7$ nm). The total multilayer thickness t was, in all cases, equal to 100 nm. A schematic representation of the systems studied is shown in Fig. 1.

Several authors[6,34–36] have applied the calculus of variations to minimize the total free energy density in stripe-domain films in order to find the more stable configuration of the magnetization. Recently, magnetic reversal processes and coercivity in ultrathin films with perpendicular surface anisotropy have been studied using a continuum micromagnetic model.[37] However, to the best of our knowledge, the calculation of $\chi_{t\beta}^{-1}$ in the presence of stripe domains does not seem to have been discussed previously. Here we present a micromagnetic calculation[38,39] of such a problem. Good agreement is found between theory and experiment, as we shall see below.

II. TRANSVERSELY BIASED INITIAL SUSCEPTIBILITY

We measured the field dependence of $\chi_{t\beta}^{-1}$ by means of the transverse magneto-optic Kerr effect (TMOKE). The experimental setup has been described before;[18] briefly, a light beam falls onto the film surface at $\vartheta=60°$, the incoming light being polarized in the plane of incidence (p polarization), whereas two simultaneous in-plane fields, as shown in Fig. 2, are applied orthogonally to each other, namely, a dc biasing field $\mathbf{H}$ and an ac low field $\mathbf{H}_t$, probing magneto-optically the in-plane component of magnetization; precisely speaking, $\mathbf{H}_t$ probes the component of in-plane magnetization along $\mathbf{H}_t$, such a component being perpendicular to the incidence plane of light. Conceptually, this is the definition of TBIS. The corresponding TMOKE signal is detected, at $T=300$ K, by two photodiodes whose energy windows have a maximum resolution at 1.377 eV. Thus TBIS is defined as

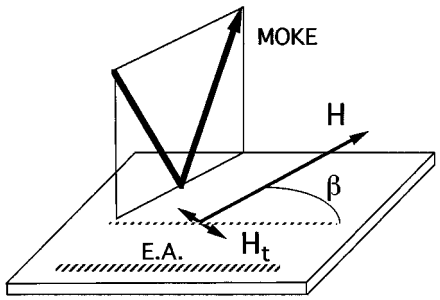

FIG. 2. Experimental determination (by TBIS via the MOKE) of the effective field acting on the mean in-plane magnetization. Here $\mathbf{H}$ is the dc bias field, and $\mathbf{H}_t$ is the ac sensing field.

$$\chi_{t\beta}(\mathbf{H})\equiv\lim_{\Delta H_t\to 0}\frac{\Delta(M\cos\theta\sin\varphi)}{\Delta H_t}. \tag{1}$$

Here β refers to the angle between the bias field $\mathbf{H}$ and the easy axis of in-plane macroscopic uniaxial anisotropy (see Fig. 2), and $M\cos\theta\sin\varphi$ is the in-plane component of magnetization along the direction of $\mathbf{H}_t$. The angles θ and φ are defined in Fig. 3. This method allows one to follow the magnetization processes. On the other hand, as well known from the micromagnetic theories of ripple developed by Harte[40] and Hoffmann,[41] if M is in the film plane *and* the thin-film fine-scale inhomogeneity case[40] is valid, then the field dependence of inverse TBIS $\chi_{t\beta}^{-1}$ follows:[42]

$$\chi_{t\beta}^{-1}(H)\cong a(H\pm H_{Ku})+b(H\pm H_{Ku})^{-1/4}+c(H\pm H_{Ku})^{-1}, \tag{2}$$

where $\beta=0$ (H applied along the easy axis), $\beta=\pi/2$ (H applied along the hard axis), and H_{Ku} is the effective field of macroscopic uniaxial anisotropy in the film plane. The first term on the right-hand side of Eq. (2) corresponds to the *coherent-rotation* process (Stoner-Wohlfarth model), the second one is the *ripple* term related to the local fluctuations in the magnetization direction, and the last one is the *skew* term due to the local fluctuations of the induced magnetic anisotropies. In the case of amorphous FeSi thin films, it has been found[15,19] that the third term on the right-hand side of Eq. (2) is negligible against the first two terms.

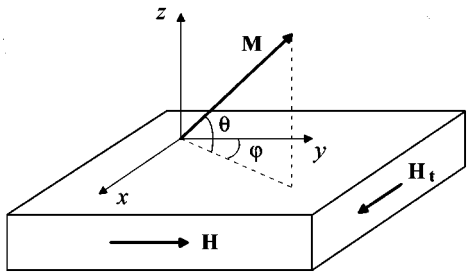

FIG. 3. Geometry of magnetization and applied fields adopted in the minimization of the free energy.

H_{Ku} is obtained from linear extrapolations[18] of the curves $\chi_{t\beta}^{-1}$ vs H, from high fields, to the values $\chi_{t0}^{-1}=0$ and $\chi_{t\pi/2}^{-1}=0$. In real films, the extrapolations of $\chi_{t\pi/2}^{-1}$ and χ_{t0}^{-1} cut the abscissa at asymmetrical points separated by $\Delta H=2H_K$. This asymmetry[18] is due to the ripple term, and hence, it is proportional to the value of b. Extensive studies of the b and c coefficients have been published elsewhere.[18,19] In particular, the b coefficient yields valuable physical information about the local anisotropy constant $K_{\rm loc}$ of a random distribution of local easy axes.[42–44] For $3d$ ions in amorphous materials, $K_{\rm loc}$ can be[19,44] in the range 10^5 J/m^3 $<K_{\rm loc}\leqslant 10^6$ J/m^3 corresponding to correlation lengths of 2 nm $>d\geqslant 0.25$ nm. Note that $d\approx 0.25$ nm is related to the atomic volume V in the framework of the Harris-Plischke-Zuckermann (HPZ) model[45] for amorphous magnetism. This order of magnitude for $K_{\rm loc}$ will be considered below as a possible source for perpendicular anisotropy, because of the anisotropic atomic coordination of nearest neighbors at very low modulation lengths λ.

The validity of the ''thin-film fine-scale inhomogeneity approximation,'' [40] in a given sample, is restricted by the particular values of exchange stiffness, dipolar coupling forces, and the shape and volume of the small regions with homogeneous local anisotropy. In a polycrystalline film, the latter correspond to the crystallites.[40]

Typical experimental maximum values of H and H_t are $H\approx 10H_{Ku}$ and $H_t\approx 10^{-2}H_{Ku}$, i.e., 10 times higher and 100 times lower than the anisotropy field, respectively.

III. MICROMAGNETIC CALCULATION OF TBIS ($\chi_{t\beta}$) IN STRIPE-DOMAIN FILMS

We studied theoretically the behavior of TBIS from a micromagnetic point of view, in order to explain the $\chi_{t\beta}^{-1}$ curves when stripe domains are present. We analyzed several models for the profile of the out-of-plane angle of magnetization, viz., trapezoidal, sawtooth, and sine wave. The latter was found to give the more stable magnetization arrangement, and we shall describe it here.

Let us consider a thin film *isotropic* in the basal plane, its film thickness being $t>t_c$.

Step 1: nonzero bias field and zero alternating field: $\mathbf{H}\neq\mathbf{0}$ and $\mathbf{H}_t=\mathbf{0}$. In the one-dimensional model of stripe domains proposed, the xy plane is taken as the film plane, the stripe domains being directed along the y axis and the local magnetization only has components in the yz plane, according to the law $M_z(x)=M_s\sin\theta(x)$, where $\theta(x)=\theta_0\sin(\pi x/\Lambda)$ is the out-of-plane angle of the local magnetization and Λ is the stripe width. The stripe domain structure is shown in Fig. 4. The bias field **H** is applied in the film plane along the y direction; i.e., **H** is parallel to the stripes.

We found the evolution of θ_0 and Λ with H by minimizing numerically the total free energy density of the system. For other magnetization profiles, such an evolution has been calculated by other authors, as, for example, Kooy and Enz,[46] Druyvesteyn *et al.*,[35] etc., solving zero-torque equations.

The total free energy density of the system is given by

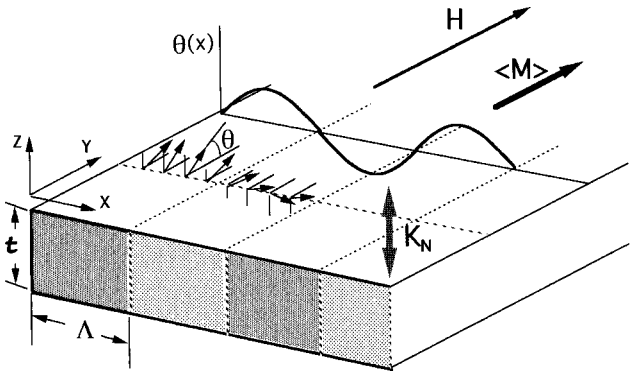

FIG. 4. Sine-wave profile of the out-of-plane angle θ of magnetization across the stripe-domain structure. A bias field **H** is applied. $\langle M\rangle$ is the mean value of magnetization along the direction of the stripes, K_N is the perpendicular anisotropy energy density, and Λ is the stripe width.

$$e=\frac{1}{2\Lambda}\int_{-\Lambda}^{\Lambda}\left\{K_N\cos^2\theta(x)+A\left(\frac{\partial\theta(x)}{\partial x}\right)^2-\vec{H}\cdot\vec{M}-\frac{1}{2}\vec{H}_D\cdot\vec{M}\right\}dx, \tag{3}$$

where K_N is the perpendicular anisotropy constant, A is the exchange stiffness, $\vec{H}$ is the applied field, $\vec{M}=M_s(0,\cos\theta(x),\sin\theta(x))$ is the local magnetization vector (see Fig. 4), and $\vec{H}_D$ is the demagnetizing field, which is calculated following the Fourier's series method proposed by Kaczer *et al.*[34] The fourth term (demagnetizing energy) is due to the magnetic free poles at the film surface as $\vec{M}$ oscillates out of the film plane.

On integration of Eq. (3), one gets

$$e=\frac{K_N}{2}[1+J_0(2\theta_0)]+A\frac{\pi^2\theta_0^2}{2\Lambda^2}-HM_sJ_0(\theta_0)+4M_s^2\sum_{\substack{n>0\\ \text{odd}}}\frac{\Lambda}{nt}J_n^2(\theta_0)(1-\exp(-n\pi t/\Lambda)). \tag{4}$$

Here J_n are the Bessel functions of the first kind and integral order n, and t is the film thickness. It is interesting to note that the expression of demagnetizing energy for our distribution $M_z(x)$, i.e., the last term of the right-hand side of Eq. (4), is equivalent to the one obtained by Druyvesteyn *et al.*[47]

Our model predicts the existence of a critical film thickness above which stripe domains do exist. The evolution of Λ and θ_0 with H is obtained once A, K_N, M_s, and t are fixed. Our results are closer to the model I of Murayama[6] [smooth variation of $M_z(x)$] than that of Druyvesteyn *et al.*,[35] who considered an abrupt variation of $M_z(x)$ (square-wave type). We found, in all cases, that the magnetization profile $M_z(x)$ here proposed is energetically more favorable than that proposed by Druyvesteyn *et al.*[35] In general, the effect of increasing H is mainly to reduce the out-of-plane angle θ and to slightly decrease the value of Λ with respect to its zero-field value $\Lambda(H=0)$. The small change of Λ is due to the opposite effects of the exchange and demagnetizing energy.

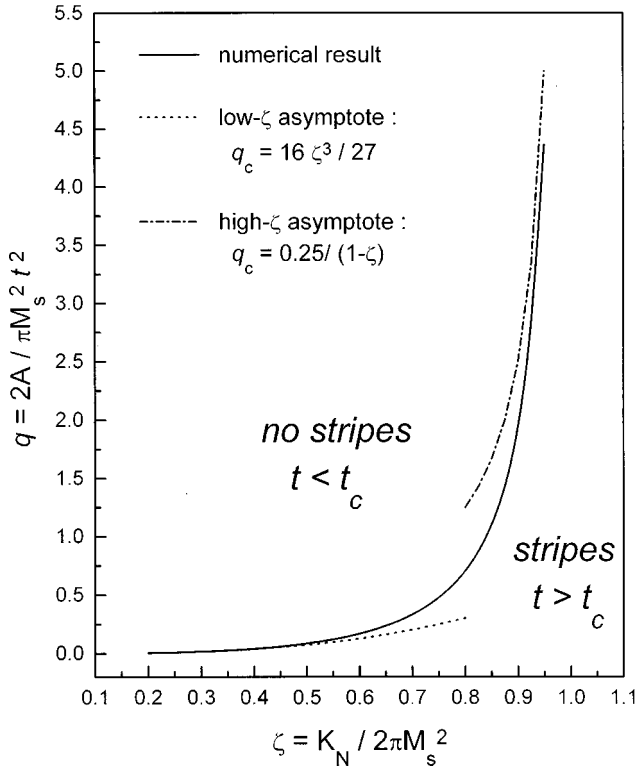

FIG. 5. Domains structure transition. As seen, stripes can exist even when $K_N < 2\pi M_s^2$.

The value of the saturation field H_s (field above which the stripes disappear; i.e., M is in the basal plane) is also obtained numerically.

From the numerical minimization of Eq. (4), it is possible to analyze the criteria for the occurrence of stripe domains. This is shown in Fig. 5, where we plot the parameter q versus ζ, here $q = 2A/\pi M_s^2 t^2$ and $\zeta = K_N/2\pi M_s^2$. It is seen that stripe domains may arise even when $K_N < 2\pi M_s^2$. The critical curve ($q = q_c$) separates the cases of *stripes* ($t > t_c$) and *no stripes* ($t < t_c$). In Fig. 5 we depict the numerical results along with the lower and upper asymptotes: $q_c = \frac{16}{27}\zeta^3$ and $q_c = 0.25(1-\zeta)^{-1}$, respectively. It should be noted that our lower asympote agrees with that obtained by Murayama[6] in his model I: $\theta = \theta(x)$.

Step 2: Nonzero bias field and nonzero alternating field $\mathbf{H} \neq 0$ and $\mathbf{H}_t \neq 0$ (conditions when measuring TBIS). Here both fields $\mathbf{H}$ and $\mathbf{H}_t$ are applied in the film plane (xy). The bias field $\mathbf{H}$ is applied along the y direction, while the ac sensing (tickle) field with amplitude H_{tm} is applied along the x axis.

The small $\mathbf{H}_t$, when applied simultaneously with the bias field $\mathbf{H}$, causes the magnetization vector to have an small azimuthal quasistatic angle $\varphi(x)$, as indicated in Fig. 6.

It should be noted that the existence of $\varphi(x)$ may give rise to variations in both the demagnetizing and the exchange energy. Let discuss here two extreme cases.

Let $\varphi(x) = \varphi_0 = \text{const}$, so that $\nabla \cdot \mathbf{M} \neq 0$. In this case there are magnetic free poles within the volume, and thus there will be a change in demagnetizing energy, even though there is no variation in the exchange energy. The magnetization has the components

$$\mathbf{M} = M_s(\cos\theta(x)\sin\varphi_0,\ \cos\theta(x)\cos\varphi_0,\ \sin\theta(x)), \quad (5)$$

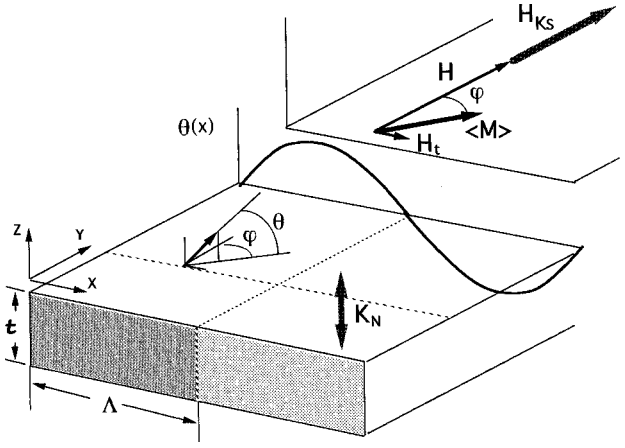

FIG. 6. When measuring TBIS, the alternating field $\mathbf{H}_t$ adds an azimuthal variation φ to the out-of-plane magnetization angle. Here $\mathbf{H}_{Ks}$ is the pseudo-uniaxial-anisotropy field associated with the stripe domains direction.

where φ_0 is the angle between $\langle M \rangle$ in the film plane and the stripes direction, as shown in Fig. 6.

Again, we calculated the new demagnetizing energy per unit volume corresponding to the magnetization distribution of Eq. (5) following the Fourier's series method proposed by Kaczer *et al.*[34] and we obtain

$$e_D(\theta_0, \Lambda, \varphi_0) = 4M_s^2 \Bigg\{ \sum_{\substack{n>0 \\ \text{odd}}} \frac{\Lambda}{nt} J_n^2(\theta_0)[1 - \exp(-n\pi t/\Lambda)] + \sin^2\varphi_0 \sum_{\substack{m>0 \\ \text{even}}} J_m^2(\theta_0) \Bigg(\pi - \frac{\Lambda}{mt} \times [1 - \exp(-m\pi t/\Lambda)] \Bigg) \Bigg\}. \quad (6)$$

The first term of the right-hand side of Eq. (6) is the demagnetizing energy in the absence of alternating field $\mathbf{H}_t$ and, as expected, such a first term agrees with the fourth term of the right-hand side of Eq. (4). The second term of the right-hand side of Eq. (6) is due to the alternating field $\mathbf{H}_t$, and it is the excess of demagnetizing energy (magnetic free poles in the volume) when the magnetization deviates an angle φ_0 from the stripe domains direction. In other words, the demagnetizing energy [Eq. (6)] has the two contributions

$$e_D(\theta(x), \varphi(x)) = e_{D\ \text{surface}}(\theta(x)) + e_{D\ \text{volume}}(\theta(x), \varphi(x)). \quad (7)$$

Note that the second term of the right-hand side of Eqs. (6) and (7) can be expressed as

$$e_{D\ \text{volume}} \equiv K_D(\theta_0, \Lambda)\sin^2\varphi_0, \quad (8)$$

and therefore, it can be seen as a *pseudo-uniaxial anisotropy* having its easy axis along the stripe-domain direction. The corresponding anisotropy ''constant'' K_D depends upon the applied field H through the changes of θ_0 and Λ. It is evident that an effective field can be associated with this anisotropy constant in order to explain the TBIS results. Taking into account that TBIS is *not* a local measurement, but it refers to

the behavior of the *in-plane* component of the mean magnetization of the thin film, Eq. (1) can be rewritten as

$$\begin{aligned}\chi_t &\equiv \partial\langle M_x(x)\rangle/\partial H_t = \partial\langle M_s\cos\theta(x)\sin\varphi(x)\rangle/\partial H_t \\ &= \partial M_s J_0(\theta_0)\langle\sin\varphi(x)\rangle/\partial H_t \approx M_s J_0(\theta_0)\partial\langle\varphi(x)\rangle/\partial H_t \\ &\approx M_s J_0(\theta_0)\partial\varphi_0/\partial H_t, \end{aligned} \tag{9}$$

where we have assumed that $\varphi(x)$ is small (as the TBIS measurement requires). In order to obtain $\varphi_0(H_t)$, we apply the perturbation theory to the local torque, taking into account all its contributions (demagnetizing, exchange, Zeeman, and anisotropy terms). For H_t small enough (condition when measuring TBIS), it is found that θ_0 and Λ do not change with respect to their values calculated above in the step 1 ($\mathbf{H}\neq 0$ and $\mathbf{H}_t=0$). In this case, φ_0 becomes

$$\varphi_0 = \frac{H_t}{H + 2K_D/\langle M_y(x)\rangle}, \tag{10}$$

where $\langle M_y(x)\rangle = M_s J_0(\theta_0)$ is the projection of the mean magnetization along the stripe-domain direction. On substitution of Eq. (10) into the last expression of Eq. (9), one gets the transverse susceptibility

$$\chi_t \approx \frac{M_s J_0(\theta_0)}{H + 2K_D/M_s J_0(\theta_0)}. \tag{11}$$

It is evident from Eq. (11) that the net field acting on $M_s J_0(\theta_0)$ consists of both the applied field H and the term $2K_D/M_s J_0(\theta_0)$ corresponding to the effective pseudo-uniaxial-anisotropy field associated with the stripe domains direction:

$$H_{Ks} = \frac{2K_D}{\langle M_y(x)\rangle}. \tag{12}$$

Then H_{Ks} is easily obtained combining Eqs. (8) and (12) with the second term of the right-hand side of Eq. (6):

$$H_{Ks} = 8M_s \sum_{\substack{m>0 \\ m \text{ even}}} \frac{J_m^2(\theta_0)}{J_0(\theta_0)} \left(\pi - \frac{\Lambda}{mt}[1-\exp(-m\pi t/\Lambda)] \right), \tag{13}$$

which can be approximated by

$$H_{Ks} \approx 8M_s \frac{J_2^2(\theta_0)}{J_0(\theta_0)} \left(\pi - \frac{\Lambda}{2t}[1-\exp(-2\pi t/\Lambda)] \right). \tag{14}$$

As expected, the magnitude of H_{Ks} depends upon H through θ_0 and Λ. As we shall show below, H_{Ks} decreases with increasing H (i.e., $\langle M\rangle$ rotates easier as the number of volume magnetic free poles decreases), and it vanishes for values of H high enough as to make the stripes disappear.

Let $\varphi(x)$ so that $\nabla\cdot\mathbf{M}=0$. In this case, when applying the alternating field, there is a variation in the exchange energy. However, the demagnetizing energy remains constant. Then, for small $\varphi(x)$, the condition $\nabla\cdot\mathbf{M}=0$, for the magnetization we consider [Eq. (5)], yields

$$\cos\,\theta(x)\varphi(x) = \text{const} \equiv \varphi_m, \tag{15}$$

where φ_m is the value of $\varphi(x)$ when $\theta(x)=0$ (i.e., when the local magnetization is in the film plane).

The exchange energy is now expressed as

$$e_A = \frac{A}{2\Lambda}\int_{-\Lambda}^{\Lambda} \left\{ \left(\frac{\partial\theta(x)}{\partial x}\right)^2 + \left(\frac{\partial\varphi(x)}{\partial x}\right)^2 \cos^2\theta(x) \right\} dx. \tag{16}$$

On substitution of Eq. (15) into Eq. (16), the latter reduces to

$$\begin{aligned} e_A &= A\,\frac{\pi^2\theta_0^2}{\Lambda^3}\int_0^{\Lambda} \cos^2\left(\frac{\pi x}{\Lambda}\right)\left\{1+\varphi_m^2\tan^2\left[\theta_0\sin\left(\frac{\pi x}{\Lambda}\right)\right]\right\} dx \\ &= A\,\frac{\pi^2\theta_0^2}{2\Lambda^2} + \left\{ A\,\frac{\pi^2\theta_0^2}{\Lambda^3}\int_0^{\Lambda}\cos^2\left(\frac{\pi x}{\Lambda}\right) \right. \\ &\quad \left. \times\tan^2\left[\theta_0\sin\left(\frac{\pi x}{\Lambda}\right)\right] dx \right\}\varphi_m^2. \end{aligned} \tag{17}$$

The first term of Eq. (17) is the exchange energy in the absence of alternating field $\mathbf{H}_t$, and, as expected, it is the same as the second term in Eqs. (3) and (4). The second term of Eq. (17) corresponds to the excess of exchange energy resulting from $\partial\varphi(x)/\partial x\neq 0$.

Note that the second term of Eq. (17) can also be expressed as

$$e_A \equiv K_A(\theta_0,\Lambda)\varphi_m^2; \tag{18}$$

then, it can be seen as an exchange-driven *pseudo-uniaxial anisotropy* having its easy axis along the stripe-domain direction.

In this case, the transverse susceptibility is

$$\begin{aligned}\chi_t &\equiv \partial\langle M_x(x)\rangle/\partial H_t = \partial\langle M_s\cos\theta(x)\sin\varphi(x)\rangle/\partial H_t \\ &\approx \partial\langle M_s\varphi(x)\cos\theta(x)\rangle/\partial H_t \approx M_s\partial\varphi_m/\partial H_t, \end{aligned} \tag{19}$$

where the last step results on setting the condition given by Eq. (15).

In order to obtain $\varphi_m(H_t)$, again we apply the perturbation theory to the local torque, taking into account all its contributions (demagnetizing, exchange, Zeeman, and anisotropy terms), in a similar way as we did before when we obtained Eq. (10). The calculation yields

$$\varphi_m = \frac{H_t}{g(\theta_0)H + 2K_A/M_s}, \tag{20}$$

where the function $g(\theta_0)$ is found to relate φ_m to the mean value of $\varphi(x)$:

$$\langle\varphi(x)\rangle = \frac{1}{\Lambda}\int_0^{\Lambda}\frac{\varphi_m}{\cos(x)}\,dx = \varphi_m g(\theta_0). \tag{21}$$

Once we determine φ_m and considering that $g(\theta_0)J_0(\theta_0) \cong 1$, the transverse susceptibility can be rearranged as

$$\chi_t \approx \frac{M_s J_0(\theta_0)}{H + 2K_A J_0^2(\theta_0)/M_s J_0(\theta_0)}. \tag{22}$$

Again, we can define an effective *pseudo-uniaxial-anisotropy field* H_{Ks} associated with the stripe-domain direc-

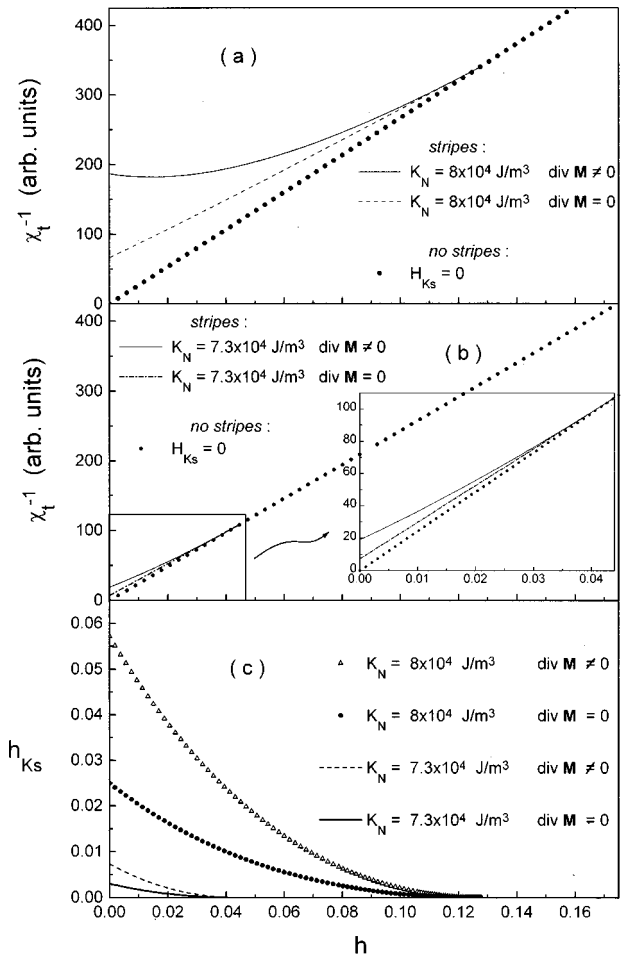

FIG. 7. Theoretical curves for (a) and (b) $\chi_{t\beta}^{-1}$ vs h ($h=H/H_{KN}$, $H_{KN}=2K_N/M_s$); (c) h_{Ks} vs h, where $h_{Ks}=H_{Ks}/H_{KN}$ is the normalized pseudo-uniaxial-anisotropy field. All of these curves were calculated considering $M=600$ emu/cm^3, $A=10^{-6}$ erg/cm, and $t=100$ nm.

tion, in a similar way as done above for the case $\nabla\cdot\mathbf{M}\neq 0$. For expression (22) such a *pseudo-uniaxial-anisotropy field* corresponds to the term $2K_AJ_0^2(\theta_0)/M_sJ_0(\theta_0)$.

On combining Eqs. (17), (18), and (22),

$$H_{Ks}=\frac{2AJ_0(\theta_0)}{M_s}\frac{\pi^2\theta_0^2}{\Lambda^3}\int_0^{\Lambda}\cos^2\left(\frac{\pi x}{\Lambda}\right)\tan^2\left[\theta_0\sin\left(\frac{\pi x}{\Lambda}\right)\right]dx. \tag{23}$$

H_{Ks} depends upon the applied field H through the changes of θ_0 and Λ. As in the case $\nabla\cdot\mathbf{M}\neq 0$, H_{Ks} decreases with increasing H due mainly to the changes in θ_0. The evolution of θ_0 and Λ with H is the same as in the above step 1.

In order to show the behavior of both free-pole-driven or exchange-driven χ_t and H_{Ks}, given by Eqs. (11), (14) and (22), (23), respectively, let us set some values of the parameters A, M_s, K_N, and t into the expressions for χ_t and H_{Ks}. To illustrate this, we will choose typical values of *homogeneous* FeSi thin films 100 nm thick:[19] $M_s=600$ emu/cm^3, $A=10^{-6}$ erg/cm, and $K_N\sim 10^6$ erg/cm^3. In Fig. 7 we show the results for χ_t^{-1} and h_{Ks} as a function of h (where $h=H/H_{KN}$, $H_{KN}=2K_N/M_s$, and $h_{Ks}=H_{Ks}/H_{KN}$). Figures 7(a) and 7(b) show the high sensitivity of our model to changes in K_N for both cases magnetic free poles ($\mathrm{div}\,\mathbf{M}\neq 0$) or exchange ($\mathrm{div}\,\mathbf{M}=0$). As seen in Figs. 7(a), 7(b), and 7(c), saturation, i.e., vanishing stripe-domain structure, can be reached at $h=h_s=0.04$ and 0.13, for $K_N=7.3\times10^4$ J/m^3 (7.3×10^5 erg/cm^3) and $K_N=8\times10^4$ J/m^3 (8×10^5 erg/cm^3), respectively. The latter values of h_s (0.04 and 0.13) correspond to saturating applied fields of $H_s\approx 100$ Oe and $H_s\approx 350$ Oe, respectively.

Additionally, for fixed values of M_s, K_N, K_u, and A, the theory shows an increase of H_S for increasing t, which actually has been experimentally observed.[48] This conclusion is similar to that reported by Murayama.[49] Thus, in the context of our theoretical model, such a variation of H_s upon t could be used to determine K_N.

Which of the cases $\nabla\cdot\mathbf{M}\neq 0$, $\nabla\cdot\mathbf{M}=0$, or an intermediate one is energetically more favorable depends upon the particular values of the parameters A, M_s, K_N, and t. For the values we chose to calculate the curves of Fig. 7, the lower energy corresponds to the second case ($\nabla\cdot\mathbf{M}=0$).

Effect of existing in-plane uniaxial anisotropy K_u. As already pointed out in our above discussion, we did not consider any anisotropy in the film plane. However, real films may well have both perpendicular K_N and in-plane K_u uniaxial anisotropies. Here only the case when K_u is fairly small as compared to K_N is considered, but obviously it is not a necessary condition for thin films. The existence of uniaxial anisotropy in the film plane will cause, in a first approximation, a splitting of the $\chi_{t\beta}^{-1}$-versus-H curves accompanied by shifts of $\pm H_{Ku}$ in the abscissa axis. In this way one gets the cases corresponding to χ_{t0}^{-1} and $\chi_{t\pi/2}^{-1}$. The intuitive justification of these results is immediate given that $\chi_{t\beta}^{-1}$ is proportional to the effective field acting on the mean magnetization. In the case corresponding to Fig. 7 (lack of *in-plane* uniaxial anisotropy H_{Ku}), the effective field is only given by the sum of the bias field $\mathbf{H}$ and the contribution of the stripe domain structure $\mathbf{H}_{Ks}$. Likewise, for $\chi_{t\beta}^{-1}$ the effective field acting on the mean *in-plane* magnetization is given by $H^{\mathrm{eff}}=H+H_{Ku}+(H_{Ks})_0$ for χ_{t0}^{-1} and $H^{\mathrm{eff}}=H-H_{Ku}+(H_{Ks})_{\pi/2}$ for $\chi_{t\pi/2}^{-1}$, with the uniaxial anisotropy field H_{Ku} being in the film plane.

The H dependence of $(H_{Ks})_0$ is simply obtained replacing H with $H+H_{Ku}$. On the contrary, the exact H evolution of $(H_{Ks})_{\pi/2}$ is rather difficult, because it requires to put K_u into the expression of the total free energy to be minimized in order to get $\varphi(H_t)$.

From the above discussion about the evolution of $(H_{Ks})_0$ with H, it is deduced that the corresponding saturation field is $(H_s)_0=H_s-H_{Ku}$. On the other hand, for fields applied perpendicularly to the in-plane easy axis the saturation field is $(H_s)_{\pi/2}\approx H_s$ because including K_u in the total free energy does not affect the results of the above step 1 (i.e., $H\neq 0$ and $H_t=0$), provided that $H>H_{Ku}$, as usually found, because the saturation field H_s is higher than H_{Ku} for the low value of K_u relative to K_N [note that $K_u\approx 10^3-10^4$ erg/cm^3 (10^2-10^3 J/m^3) and $K_N>10^5$ erg/cm^3 (10^4 J/m^3)].

IV. EXPERIMENTAL STUDY OF TBIS IN STRIPE-DOMAIN FeSi THIN FILMS AND FeSi/Si MULTILAYERS

A. Sample preparation

Both amorphous Fe_xSi_{1-x} thin films and amorphous Fe_xSi_{1-x}/Si multilayers were prepared. Amorphous Fe_xSi_{1-x} thin films were grown by dc triode sputtering ($p_{Ar} \simeq 10^{-4}$ Torr) on glass substrates, held at room temperature. Two independent cathodes of Fe and Si were used. They were polarized with voltages V_{Fe} and V_{Si}. The ''thin films'' studied were thick enough (150 nm) as to be regarded *homogeneous* in composition. The value of x is fixed by a previous calibration of V_{Fe} and V_{Si}. On the other hand, five series of Fe_xSi_{1-x}/Si multilayers ($0.68 \leqslant x \leqslant 0.82$) were prepared, each series having five different values of *nominal* modulation lengths (λ) ranging from 7 to 0.4 nm. During sample preparation, V_{Si} was held constant, whereas $V_{Fe}(t)$ was varied between V_{Fe} maximum and zero as a square wave. The value of maximum V_{Fe} determines x for a given series, while the period of V_{Fe} determines the value of λ for the multilayer. In this way the average Fe content $\langle x \rangle$ remains constant across each series. In all cases, the total multilayer thickness t was close to 100 nm, as shown in Fig. 1. The composition $\langle x \rangle$ was checked by electron probe x-ray microanalysis (EMPA) using, as standards, homogeneous FeSi films with a wide range of compositions and film thicknesses.

B. Experimental results and discussion

1. Homogeneous Fe_xSi_{1-x} thin films

In Fig. 8(a) we show the $\chi^{-1}_{t\pi/2}$ behavior for a $Fe_{0.65}Si_{0.35}$ thin film of 150 nm in thickness. An abrupt slope change is observed, the latter being associated with the stripe-domain structure. Such behavior has been observed before, as, for example, in NdFeB (Ref. 50) and FeSi (Ref. 19) thin films. Moreover, in Ref. 19 it was shown that such an abrupt change cannot be explained only by ripple. In fact, the ripple contribution can be separated from that of stripe domains using a $(h-1)^{1/4}\chi^{-1}_{t\beta}$-versus-$(h-1)^{5/4}$ plot,[18] as Eq. (2) suggests. Notice that, as pointed out in the above Sec. II, the coefficient b of Eq. (2) is related to the magnetization ripple, and it is obtained using the extrapolation of the data from high fields to the value of $(h-1)^{5/4} \rightarrow 0$. As seen in Fig. 8(b), ripple cannot account for the whole set of points because of the departure from linearity for $h < h_s$. It should be stressed again here that Hoffmann's model is valid only for $h > h_s$, i.e., only when M lies *in the film plane*.

If we take $H_s \approx 150$ Oe for this sample, on setting $M_s = 620$ emu/cm^3, $A = 10^{-6}$ erg/cm (10^{-11} J/m), and $t = 150$ nm, we obtain $K_N = 10^5 - 10^6$ erg/cm^3 ($= 10^4 - 10^5$ J/m^3), and a critical thickness of $t_c \approx 133$ nm: then, $t > t_c$ and our model agrees with experiment: Stripes do appear.

On the other hand, as assumed in Sec. III, our model does not include the possibility of ripple contributions; however, in real films both stripe domains and ripple may coexist.[10] The ripple term means that modulation of the magnetization is present along the y direction, and it is related to the size of the *coupling volumes* predicted in Hoffmann's model.[41,43]

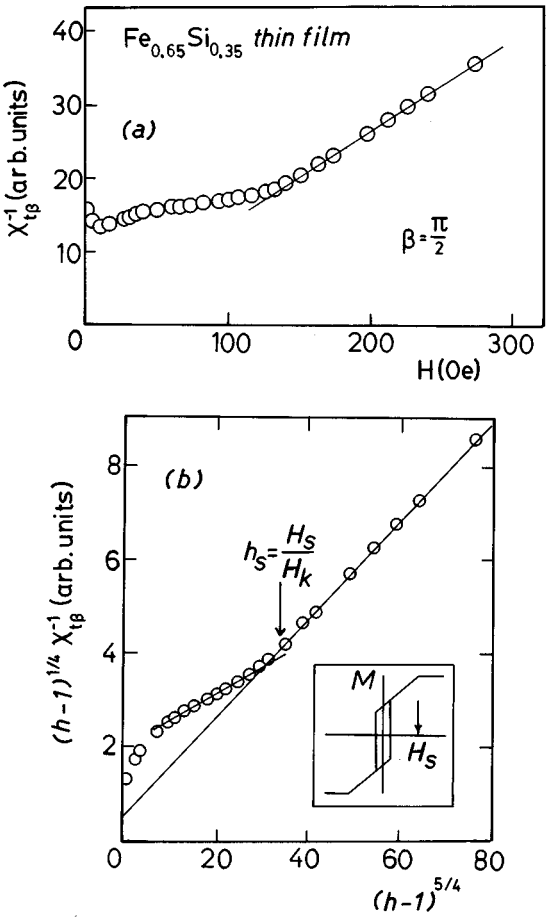

FIG. 8. (a) Experimental $\chi^{-1}_{t\beta}$ data for a *homogeneous* stripe-domain FeSi thin film of 150 nm in thickness, at $T = 300$ K. (b) Separation of ripple from stripes contributions to $\chi_{t\beta}$ for the same sample as in the above panel. For $h > h_S$, M_s is *in the film plane*.

Given that real films may show ripple, it is expected that, for a given field H, the amplitude of the magnetization ripple for χ_{t0} will be lower than that for $\chi_{t\pi/2}$, and therefore, the theoretical result will be closer to the experimental behavior of χ_{t0}. Thus our model will be more reliable for χ_{t0}. Then, in order to get K_N, the experimental values of H_{s0} and H_{Ku} should be used.

2. Fe_xSi_{1-x}/Si multilayers

In Figs. 9(a) and 9(b) we show two representative cases of the field dependence of $\chi^{-1}_{t\beta}$ against λ for the series with $x = 0.76$ and $\lambda = 6.6$ nm and $\lambda = 0.4$ nm, i.e., the extreme values of *nominal* λ within this series. In both cases, $\chi^{-1}_{t\beta}$ vs H is obtained decreasing the value of H from the saturated state.

a. Multilayers without stripe domains. The behavior of $\chi^{-1}_{t\beta}$ versus H observed for $\lambda = 6.6$ nm [Fig. 9(a)] corresponds to the one typically found in homogeneous amorphous thin films with low magnetization ripple and no stripe domains, i.e., a quasilinear behavior for $\beta = 0$ and a minimum in the vicinity of $H = H_k$ for $\beta = \pi/2$. Likewise, the same behavior was observed in multilayers with $\lambda \geqslant 5$ nm and $0.68 < x < 0.82$.

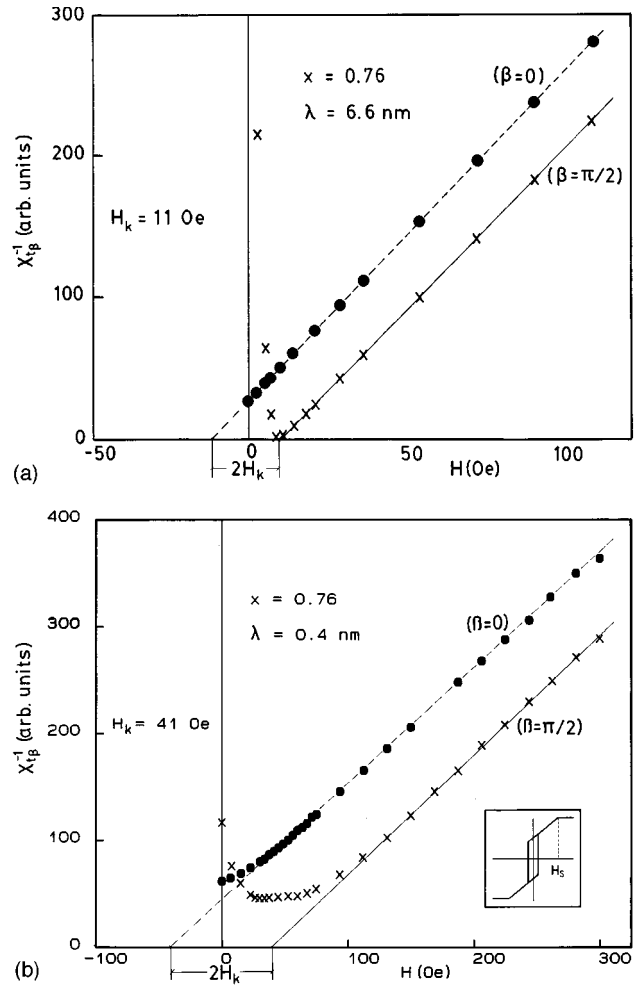

FIG. 9. Experimental $\chi_{t\beta}^{-1}$-H curves for multilayers of $Fe_{0.76}Si_{0.24}$/Si at $T=300$ K: (a) $\lambda=6.6$ nm. Here no stripes are observed. K_N might be present; however, M is *not tilted* out of the film plane; (b) $\lambda=0.4$ nm. This is the typical case in which stripe domains, and hence, perpendicular anisotropy are present. Here M is *tilted* out of the film plane. The saturation field is $H_s \approx 110$ Oe. The inset shows the *transcritical* hysteresis loop, which is associated with perpendicular anisotropy.

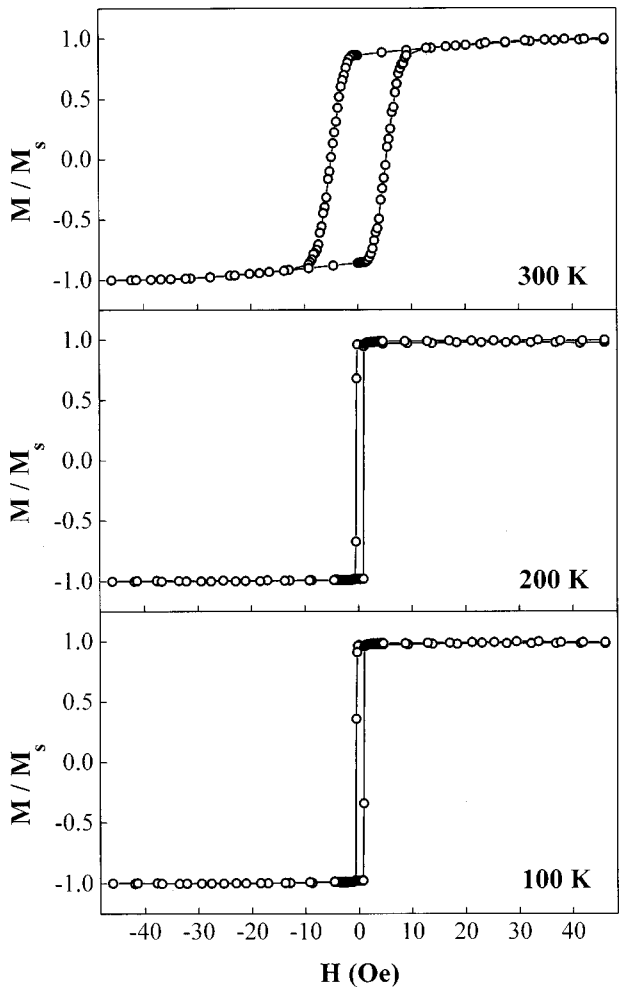

FIG. 10. Experimental temperature evolution of the TMOKE-hysteresis loops in $Fe_{0.71}Si_{0.29}$/Si multilayers with $\lambda=0.4$ nm, showing stripe domains. At $T=200$ K and $T=100$ K, M_s lies *in the film plane* (no transcritical loop), whereas M_s is *out of the plane* at $T=300$ K.

b. Multilayers with stripe domains. On the contrary, for $\lambda=0.4$ nm [Fig. 9(b)], a sharp slope change shows up in both χ_{t0}^{-1} and $\chi_{t\pi/2}^{-1}$ for applied fields quite different from H_{Ku}. Note that $H_s > H_{Ku}$. Again, such a pronounced change cannot be explained by realistic values of magnetization ripple.[18,19] In each case, the extrapolations of χ_{t0}^{-1} and $\chi_{t\pi/2}^{-1}$ from high fields to the values of $\chi_{t0}^{-1}=0$ and $\chi_{t\pi/2}^{-1}=0$ cut the abscissa axis at points separated by $\Delta H=2H_{Ku}$. In addition, this sample presents *transcritical* hysteresis loops [see inset of Fig. 9(b)], better observed when **H** is applied along the hard axis of in-plane magnetization ($\beta=\pi/2$), in agreement with the TBIS curves. Similar behaviors (stripe domains and transcritical loops) have been observed for multilayers in the very-low-modulation-length regime ($\lambda \leqslant 0.8$ nm) and $x \leqslant 0.71$.

Additionally, in Fig. 10 we show the temperature evolution of the hysteresis loops obtained by MOKE in $Fe_{0.71}Si_{0.29}$/Si multilayers with $\lambda=0.4$ nm, presenting stripe domains. An interesting temperature-dependent phenomenon is observed: The transcritical loop shows up at $T=300$ K, but it vanishes at $T=200$ K and $T=100$ K. Moreover, the coercive fields H_c associated with transcritical loops are higher than those of nontranscritical loops. This thermal evolution of the coercivity cannot be explained by domain-wall displacement mechanisms. But the extinction of transcritical loops may be understood by taking into account that M_s increases for decreasing temperature. For example, for the multilayer $Fe_{0.71}Si_{0.29}$/Si, a gradient[51] of $\Delta M_s/\Delta T \approx -0.15$ emu g_{Fe}^{-1} K^{-1} has been determined for the range $100 < T < 300$ K. Likewise, Fig. 10 indicates that M_s is *in the plane* at $T=200$ K and $T=100$ K and *out of the plane* at $T=300$ K. In addition to that, Fig. 10 supports the stated link between stripe domains and transcritical loops, as mentioned in the Introduction.

In order to verify the nominal modulation length, we performed x-ray-diffraction experiments. The Cu $K\alpha_1$ line energy ($\lambda=1.5405$ Å) was used as a source of soft x rays. The scanning rate was 0.005 deg/s. In Fig. 11 we show the x-ray-diffraction patterns for the same samples discussed in Fig. 9. No multilayer structure was detected for $\lambda=0.4$ nm [Fig. 11(a)], whereas a sharp multilayer structure is observed for

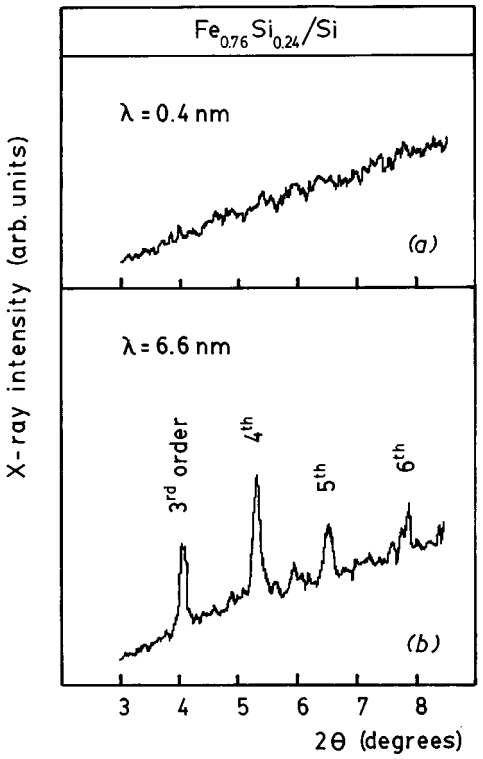

FIG. 11. X-ray-diffraction patterns for the same multilayer systems as in Fig. 9: (a) For $\lambda = 0.4$ nm, no multilayer structure is detected; (b) a sharp multilayer structure is observed for $\lambda = 6.6$ nm. The Cu K_{α_1} line energy ($\lambda = 1.5405$ Å) was used as a source of soft x rays.

$\lambda = 6.6$ nm [Fig. 11(b)]. Systematically, multilayer-type structures were observed by x-ray diffraction only for values of λ higher than 3.5 nm. Below this value, we did not observe a clear modulation.[51] We conclude that only for $\lambda \leqslant 0.8$ nm and mean compositions of $\langle x \rangle \approx 0.60$, TBIS clearly shows the existence of stripes which are associated with perpendicular anisotropy, as already shown in Fig. 9(b). Thus perpendicular anisotropy in the system Fe_xSi_{1-x}/Si looks like being *not* exclusive of a well-defined multilayered structure.

We can estimate the order of magnitude of perpendicular anisotropy K_N in Fe_xSi_{1-x}/Si multilayers by setting the *experimental value* of $H_s = (H_s)_0 + H_{Ku}$ into our model along with M_s, t, and A. For example, the multilayer of Fig. 9(b) (with the *lowest modulation length* $\lambda = 0.4$ nm) has $H_s \approx 110$ Oe and $M_s = 612$ emu/cm^3;[51] for these values our model yields $K_N \approx 7.5 \times 10^5$ erg/cm^3 (7.5×10^4 J/m^3) and $t_c \approx 93$ nm; then, $t > t_c$ and stripes exist. On the contrary, the absence of stripe domains in multilayers with the *highest modulation length* $\lambda \geqslant 3.5$ nm [Fig. 9(a)] does not necessarily imply that K_N should increase as the nominal λ decreases; a simple explanation for the experimental behavior found may be given even assuming that K_N remains constant across the multilayer series. In fact, the samples with the lowest film thicknesses tend to constitute homogeneous films with mean concentrations $\langle x \rangle$ being lower than the nominal values of x for each layer. In other words, the case shown in Fig. 9(b), for $\lambda = 0.4$ nm and $x = 0.76$, may be regarded as a *homogeneous* thin film with 100 nm in thickness (because t_{magnetic} approaches t_{total}) and $\langle x \rangle = 0.61$.[51] On the other hand, the sample of the same series with $\lambda = 6.6$ nm and $x = 0.76$ does correspond to a real multilayer structure with total thickness of 100 nm and, therefore, with a lower effective magnetic thickness [($t_{\text{magnetic}} = 81$ nm) (Ref. 51)]. Note that the higher λ, the better defined the multilayer structure.

Taking into account that M_s increases with x in amorphous Fe_xSi_{1-x}/Si (Ref. 22) and that, for a given value of K_N, the critical thickness for the occurrence of stripe domains is a function of the inverse M_s (Refs. 6 and 38), one concludes that stripes are more likely to occur in the case of multilayers with low *nominal* values of λ. In Fig. 9(a), K_N might exist, but M is *not tilted* out of the film plane, whereas in Fig. 9(b), K_N exists and we detect the stripes by TBIS.

For the above discussion, even if K_N were the same in Fig. 9(a) as in Fig. 9(b), we would not detect any stripes for $\lambda = 6.6$ nm. For example, if one assumes that $K_N = 8 \times 10^4$ J/m^3, as in Fig. 7(a), and taking into account that $M(300\text{ K}) = 677$ emu/cm^3 for $x = 0.76$, our model gives a critical thickness of $t_c \approx 105$ nm for the occurrence of stripes domains. However, for this sample the *effective* $t_{\text{magnetic}} = 81$ nm. Thus no stripes are to be observed for $\lambda = 6.6$ nm, in agreement with Fig. 9(a), because $t_{\text{magnetic}} < t_c$.

Alternately, we can estimate the value of K_N that would be necessary in order to have stripe domains in this high-modulation-length multilayer; on setting $M_s(300\text{ K}) = 677$ emu/cm^3 and $t_{\text{magnetic}} = 81$ nm one obtains $K_N \geqslant 9.5 \times 10^4$ J/m^3.

3. Particular analysis of $\chi^{-1}_{t\pi/2}$

In all cases, it was found that the experimental $\chi^{-1}_{t\pi/2}$ curves change faster than the theoretical curve. What might be some causes for this difference first, ripple effects may well be present in real films and they fall outside the scope of our model; as mentioned above, ripple effects are expected to be sharper in $\chi^{-1}_{t\pi/2}$ than in χ^{-1}_{t0}; second, real films could have spin pinning, impurities, etc., impeding the magnetization to follow the ideal behavior.

As already mentioned, our model assumes quasistatic conditions, whereas the experimental determination of $\chi_{t\beta}$ is made with an alternating field H_t at a frequency of 10^3 Hz. In order to elucidate the possible influence of both amplitude and frequency of H_t on $\chi_{t\beta}$, we carried out $\chi_{t\beta}$ measurements in the range $30\text{ Hz} < \nu < 980\text{ Hz}$ and $169\text{ mOe} < H_{tm} < 592$ mOe. In Fig. 12 we show the results obtained on a stripe-domain $Fe_{0.71}Si_{0.29}/Si$ multilayer with $\lambda = 0.4$ nm. As seen, neither the slope at H_s nor the shape of the curve changes upon changing ν and H_{tm}, and we conclude that there are no dynamic effects in the range we investigated. Thus the assumption made in our model is correct.

4. Possible origins of K_N

At this point it is necessary to discuss the possible origins of the perpendicular anisotropy in the system we are studying. These are some sources of K_N.

a. Magnetoelastic coupling. The isotropic compressive stress σ, when coupled to the magnetostriction λ_s, provides a magnetoelastic[52] contribution of $\Delta K_{N\,\text{magnetoel}} = (3/2)\lambda_s\sigma$. In particular, if we use known values[31] for FeSi/Si of satu-

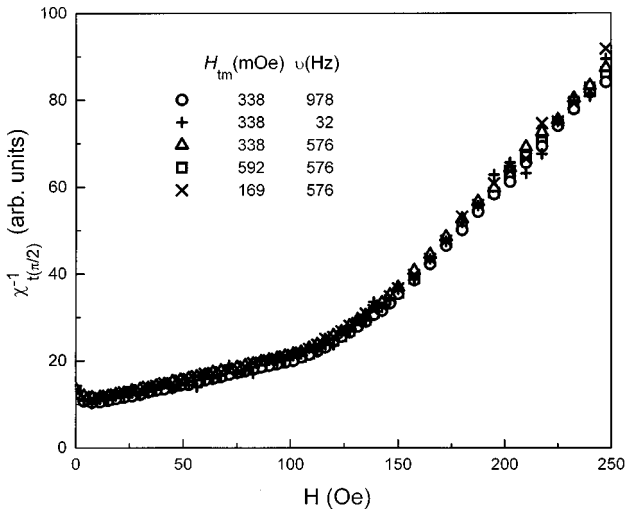

FIG. 12. Experimental $\chi_{t\beta}^{-1}$ as a function of frequency, alternating field amplitude, and bias field in $Fe_{0.71}Si_{0.29}$/Si multilayers with $\lambda = 0.4$ nm, at $T = 300$ K. All curves agree quite well. Thus there are no dynamic effects in the typical TBIS behavior of stripe-domain FeSi/Si multilayers.

ration magnetostriction $\lambda_s = 1-3\times10^{-5}$ and internal planar stresses $\sigma \approx 10^{10}$ dyn/cm^2 ($=10^9$ N/m^2); then, the magnitude of perpendicular anisotropy brought about by internal planar stress due to substrate constraint in Fe-Si sputtered multilayers is estimated to be in the range 1.5×10^4 J/m^3 $< K_N < 4.5\times10^4$ J/m^3 for mean compositions of $0.61 < \langle x \rangle < 0.75$. Thus magnetoelastic effects account for a considerable part (20%–60%) of perpendicular anisotropy in *homogeneous* FeSi/Si multilayers ($\lambda \leqslant 0.8$ nm). However, there could be other sources of perpendicular anisotropy. We cannot rule out, for example, the following.

b. Anisotropy in the atomic coordination of nearest neighbors. For nominal modulations lengths of $\lambda = 0.4$ nm and $\lambda = 0.8$ nm, no multilayered structure is observed. However, at a microscopic scale, an atomic coordination anisotropy between nearest neighbors of Fe ions may well be present in localized regions of the samples, because of the *nominal* alternating nature of FeSi and Si layers, even at very low λ values. Taking into account that very large values of $K_{\rm loc}$ for $3d$ ions can be deduced from the ripple contribution to TBIS (Ref. 19) in amorphous FeSi films (10^5 J/m$^3 < K_{\rm loc} \leqslant 10^6$ J/m^3 corresponding to correlation lengths 2 nm$> d \geqslant 0.25$ nm), a perceptible orbital contribution to the Fe magnetic moment cannot be excluded. Then anisotropic exchange or pair anisotropy can contribute to K_N if the distribution of Fe pairs is not random. In our case, because of the sample preparation method, Fe-Fe nearest-neighbor correlations are expected to be greater *in the film plane* than perpendicular to the plane, and K_N values of the order of 10^4 J/m^3 can be explained by models of bond orientational anisotropy.[53]

V. SUMMARY

We studied the behavior of transverse susceptibility $\chi_{t\beta}$ in stripe-domain thin films and multilayers. A theoretical model has been proposed in order to calculate $\chi_{t\beta}$ when stripe domains are present. We showed that there is an effective anisotropy field associated with the stripe domains. The existence of perpendicular anisotropy was found to be *not* exclusive of a well-defined multilayer structure. In the case of composition-modulated Fe_xSi_{1-x}/Si multilayers, such perpendicular anisotropy has been detected even for very low modulation lengths ($\lambda < 3.5$ nm), where a multilayer structure is not to be expected. The model proposed, combined with the experimental value of saturation field H_s, allows one to obtain both the critical thickness t_c for the occurrence of stripe domains and the perpendicular anisotropy constant K_N. The existence of the stripe domains has not been verified directly, and it would be necessary in further works to do it. For both *homogeneous* Fe_xSi_{1-x} thin films and Fe_xSi_{1-x}/Si multilayers with low modulation length, K_N was found to be $K_N = 10^4 - 10^5$ J/m^3, the latter being high enough as to explain the occurrence of stripe domains. The magnetoelastic stress contribution to the total perpendicular anisotropy ($K_N = 7.5\times10^4$ J/m^3) is estimated to be $|K_N|_{\rm magnetoel} \approx 1.5-4.5\times10^4$ J/m^3. This implies that there is an additional contribution (atomic-scale structure) to the perpendicular anisotropy; in order to confirm the as-found magnitudes of K_N and K_u it is recommended to do investigations by other techniques like torque measurements or ferromagnetic resonance. From the analysis of our earlier TBIS curves of FeSi thin films, it looks like Fe atoms exhibit some unquenched orbital momenta. Both facts (atomic-scale structure and unquenched orbital Fe momenta) become important, in light of bond orientational anisotropy models, to account for the additional contribution (of microscopic origin) to K_N.

ACKNOWLEDGMENTS

This work has been financially supported in part by the Fundación Domingo Martínez (Grant No. 4.4, 1993) and by the Spanish Government under DGICYT Grant No. MAT92-0787. One of us (L.M.A.-P.) would like to express his gratitude to the FICYT for financial support and Dr. N. C. Bobillo-Ares for fruitful discussions. We thank Dr. G. Suran (Laboratoire Louis Néel, Grenoble) for his constructive criticisms and recommendations.

*Author to whom correspondence should be addressed. Electronic address: salas@pinon.ccu.uniovi.es

[1] L. Landau and E. Lifshitz, Phys. Z. Sowjetunion **8**, 153 (1935).
[2] E. H. Kennard, Phys. Rev. **55**, 312 (1939).
[3] L. Néel, Cahiers Phys. **25**, 21 (1944).
[4] C. Kittel, Phys. Rev. **70**, 965 (1946).
[5] H. J. Williams, R. M. Bozorth, and W. Shockley, Phys. Rev. **75**, 155 (1949).
[6] Y. Murayama, J. Phys. Soc. Jpn. **21**, 2253 (1966).
[7] K. L. Chopra, *Thin Film Phenomena* (McGraw-Hill, New York, 1969), pp. 693–696.
[8] R. J. Spain, Appl. Phys. Lett. **3**, 208 (1963).
[9] N. Saito, H. Fujiwara, and Y. Sugita, J. Phys. Soc. Jpn. **19**, 1116 (1964).
[10] T. Koikeda, K. Suzuki, and S. Chikazumi, Appl. Phys. Lett. **4**, 160 (1964).

[11] S. S. Lehrer, J. Appl. Phys. **34**, 1207 (1963).
[12] A. G. Lesnik, Fiz. Met. Metalloved. **15**, 175 (1963).
[13] V. N. Pushkar', Fiz. Met. Metalloved. **17**, 158 (1964).
[14] L. S. Palatnik, L. I. Lukashenko, and A. G. Ravlik, Fiz. Tverd. Tela **7**, 2829 (1965) [Sov. Phys. Solid State **7**, 2285 (1966)].
[15] J. M. Alameda, M. C. Contreras, M. Torres, and A. González-Arche, J. Magn. Magn. Mater. **62**, 215 (1986).
[16] H. Fujiwara, Y. Sugita, and N. Saito, Appl. Phys. Lett. **4**, 199 (1964).
[17] E. J. Torok, R. A. White, A. J. Hunt, and H. N. Oredson, J. Appl. Phys. **33**, 3037 (1962); E. Feldtkeller, Z. Phys. **176**, 510 (1963).
[18] J. M. Alameda and F. López, Phys. Status Solidi A **69**, 757 (1982).
[19] J. M. Alameda, M. C. Contreras, H. Rubio, Phys. Status Solidi A **85**, 511 (1984).
[20] J. Zhang, X. B. Yang, H. Ninomiya, and H. Hoffmann, J. Magn. Magn. Mater. **131**, 278 (1994).
[21] G. T. Pérez, J. F. Fuertes, J. M. Alameda, and F. H. Salas, J. Magn. Magn. Mater. **93**, 155 (1991).
[22] J. M. Alameda, J. F. Fuertes, D. Givord, A. Liénard, B. Martínez, M. A. Moreu, and J. Tejada, J. Phys. (France) Colloq. **49**, C8-1789 (1988).
[23] J. A. Carlisle, A. Chaiken, R. P. Michel, L. J. Terminello, J. J. Jia, T. A. Callcott, and D. L. Ederer, Phys. Rev. B **53**, 8824 (1996).
[24] J. E. Mattson, S. Kumar, E. E. Fullerton, S. R. Lee, C. H. Sowers, M. Grimsditch, S. D. Bader, and F. T. Parker, Phys. Rev. Lett. **71**, 185 (1993).
[25] J. Alvarez, A. L. Vázquez de Parga, J. J. Hinarejos, J. de la Figuera, E. G. Michel, C. Ocal, and R. Miranda, Phys. Rev. B **47**, 16 048 (1993).
[26] S. Toscano, B. Briner, H. Hopster, and M. Landolt, J. Magn. Magn. Mater. **114**, L6 (1992).
[27] E. E. Fullerton, J. E. Mattson, S. R. Lee, C. H. Sowers, Y. Y. Huang, G. Felcher, S. D. Bader, and F. T. Parker, J. Magn. Magn. Mater. **117**, L301 (1992).
[28] Ch. Aron, P. Auric, and C. Jeandey, Solid State Commun. **79**, 217 (1991).
[29] X. D. Ma, Y. H. Liu, and L. M. Mei, J. Magn. Magn. Mater. **95**, 199 (1991).
[30] C. N. Afonso, A. R. Lagunas, F. Briones, and S. Girón, J. Magn. Magn. Mater. **15–18**, 833 (1980).
[31] J. A. Aboaf, R. J. Kobliska, and E. Klokholm, IEEE Trans. Magn. **MAG-14**, 941 (1978).
[32] Ph. Mangin and G. Marchal, J. Appl. Phys. **49**, 1709 (1978).
[33] Y. Shimada and H. Kojima, J. Appl. Phys. **47**, 4156 (1976).
[34] J. Kaczer, M. Zeleny, and P. Suda, Czech. J. Phys. B **13**, 579 (1963).
[35] W. F. Druyvesteyn, J. W. F. Dorleijn, and P. J. Rijnierse, J. Appl. Phys. **44**, 2397 (1973).
[36] S.-K. Chung and M. W. Muller, J. Magn. Magn. Mater. **1**, 114 (1975).
[37] X. Hu, Phys. Rev. B **55**, 8382 (1997). We thank Dr. Xiao Hu for making his article available to us prior to publication.
[38] L. M. Alvarez-Prado (unpublished).
[39] L. M. Alvarez-Prado, N. C. Bobillo-Ares, and J. M. Alameda (unpublished).
[40] K. J. Harte, J. Appl. Phys. **39**, 1503 (1968).
[41] H. Hoffmann, IEEE Trans. Magn. **4**, 32 (1968).
[42] K. Kempter and H. Hoffmann, Phys. Status Solidi **34**, 237 (1969).
[43] H. Hoffmann, Phys. Status Solidi **33**, 175 (1969).
[44] J. M. Alameda, M. C. Contreras, H. Rubio, F. Briones, D. Givord, and A. Liénard, J. Magn. Magn. Mater. **67**, 115 (1987).
[45] R. Harris, M. Plischke, and M. J. Zuckermann, Phys. Rev. Lett. **31**, 160 (1973).
[46] C. Kooy and U. Enz, Philips Res. Rep. **15**, 7 (1960).
[47] See Eq. (4) in Ref. 35.
[48] See Table 2, p. 517, in Ref. 19.
[49] See Fig. 6 in Ref. 6.
[50] J. M. Alameda, M. C. Contreras, J. F. Fuertes, A. Liénard, and F. H. Salas, J. Magn. Magn. Mater. **83**, 75 (1990).
[51] G. T. Pérez, Ph.D. thesis, Universidad de Oviedo, 1995.
[52] C. Kittel, Rev. Mod. Phys. **21**, 541 (1949).
[53] H. Fu and M. Mansuripur, Phys. Rev. B **45**, 7188 (1992).